Temperature- and field-dependent I-V characteristics of an $Ag/YBa_2Cu_3O_{7-\delta}$ fiber

W. M. Tiernan and R. B. Hallock
Laboratory for Low Temperature Physics, Department of Physics and Astronomy, University of Massachusetts, Amherst, Massachusetts 01003

(Received 2 January 1991; revised manuscript received 1 April 1991)

Temperature- and magnetic-field-dependent superconducting I-V characteristics of polycrystalline $Ag/YBa_2Cu_3O_{7-\delta}$ for current densities up to 2×10^4 A/cm^2 were investigated by means of measurements on a fiber made by the polymer-metal-complex precursor method. Data taken for $H=0.5$ G at selected temperatures from 4.3 to 85.7 K show significant changes in I-V characteristics between 85.7 and 60.8 K. Data for 0.5 G $\leq H \leq 9000$ G and $T=77.0$ K exhibit a variety of field- and current-dependent behavior, all of which is consistent with a system of weakly coupled superconducting grains. At low current levels, power-law I-V characteristics were observed for the entire range of fields, whereas at higher current levels and for $H \geq 9$ G, a crossover from power law to linear I-V behavior was seen. The I-V behavior for $H \gtrsim 9$ G is dominated by intergranular flux motion; field-dependent changes at $H \approx 60$ G suggest changes in intergranular flux flow related to single-grain lower critical fields.

I. INTRODUCTION

Polycrystalline samples of high-T_c superconductors have proven disappointing for technological applications largely because of their low critical current densities and sensitivity to small fields. Measurements of the magnetic-field-dependent drop in sample critical current (I_c) for bulk pellets[1,2] and direct measurements of the single-gain and grain-boundary critical currents in polycrystalline film samples[3] have shown that this behavior is due to Josephson-effect weak links at grain boundaries. The grain-boundary critical current has been shown to depend strongly on the relative alignment of crystal axes of adjacent grains.[4] Although low critical currents in polycrystalline samples limit their technological usefulness, these materials are nevertheless an interesting and unusual physical system. They are unusual because certain of their physical properties in the superconducting state, such as magnetization and electrical transport, can depend more on the nature and distribution of grain boundaries than on the physical properties of the material in the grains themselves.

A physical picture used to describe these materials is that of a collection of Josephson-junction-coupled superconducting grains with each grain having a uniform superconducting phase θ.[5,6] The coupling energy between grains i and j, E_{ij}, is given by

$$E_{ij}=(\hbar/2e)I_{ij}(H,T)\cos(\theta_i-\theta_j-A_{ij}) ,$$

where $I_{ij}(H,T)$ is the Josephson critical current between grains i and j and $A_{ij}=(2\pi/\phi_0)\int_i^j \mathbf{A}\cdot dl$, with $\mathbf{A}$, the magnetic vector potential and ϕ_0 the quantum of flux. The superconducting transition of such a system occurs in two steps. At a temperature T_{c0}, the single grains become superconducting. At a somewhat lower temperature T_c, there is a phase-locking transition that occurs when the coupling energy between grains is strong enough to overcome thermal fluctuations and produce phase coherence between adjacent grains. Below T_c, the sample as a whole can support a zero-voltage current. The phase-locking transition temperature T_c is expected to depend on the average grain coupling energy $\langle E_{ij}\rangle$ as $k_B T_c \sim \langle E_{ij}\rangle$. This model has been successfully used to understand the behavior of a related system, that of a fabricated two-dimensional Josephson-junction array.[7] Although these two systems share similar features, the random distribution of grain sizes and coupling energies as well as the three-dimensional distribution of grains existing in polycrystalline high-T_c materials are important differences that may have substantial effects on current-voltage (I-V) characteristics.

The I-V characteristics of these systems depend on a number of things. For small currents in zero magnetic field, a voltage arises from thermally actived "slip" of the superconducting phase between adjacent grains. This phase slip comes about because of the decrease in junction coupling energy E_{ij} as the junction current I_j approaches I_{ij}. When E_{ij} is comparable to $k_B T$, the phase difference between grains can slip due to thermal fluctuations, thereby producing a voltage, even though $I_J < I_{ij}$. The voltage developed between two grains is proportional to the time rate of phase slippage, $V=(\hbar/2e)d\theta/dt$. This effect has been well documented for single Josephson junctions[8,9] and has also been observed in fabricated Josephson-junction arrays.[7] An important consequence of this effect is that a directly measured critical current marking the onset of a measurable voltage is less than I_{ij}. For average junction currents $\langle I_J\rangle$ less than $\langle I_{ij}\rangle$, a sample's I-V characteristics are expected to be nonlinear because of thermally activated phase slippage. For $\langle I_J\rangle > \langle I_{ij}\rangle$, the I-V characteristics should become linear, with dV/dI approaching a resistance determined by the resistance of the grain boundaries. Magnetic field has two effects on the I-V characteristics. It reduces grain-boundary critical currents and also allows the pos-

sibility of a second mechanism for developing a voltage across the sample, namely, the motion of intergranular flux vortices across the sample. In two-dimensional fabricated Josephson-junction arrays, structure in the dynamic resistance dV/dI has been used to investigate the dependence of I-V characteristics on thermal phase slippage and intergranular flux motion.[7]

Near the onset of a measurable voltage, power-law I-V behavior has been observed for a number of polycrystalline samples. For bulk polycrystalline $YBa_2Cu_3O_{7-\delta}$ (Y 1:2:3) below T_{c0}, $V \propto I^a$ has been reported. The exponent a was seen to rise from 1 to ≈ 4.5 in a region ≈ 1 K below T_{c0}, and an abrupt rise in a for $a \gtrsim 1.5$ was interpreted as a precursor to the phase-locking transition.[10] In polycrystalline films made from $ErBa_2Cu_3O_{7-\delta}$ (Ref. 11) and Bi-Ca-Sr-Cu-O,[12] a somewhat different power-law behavior has been reported. In these samples, $V \propto (I - I_c)^a$ and a was found to rise from 1 to 2 in a relatively small region below T_{c0}, followed by a more gradual rise with further reduction in temperature.

The addition of silver to Y 1:2:3 has been found to increase the critical current density in polycrystalline samples.[13] Silver apparently does not go into the Y 1:2:3 lattice, but has beneficial effects on grain growth and grain-boundary weak links. In this study we report measurements of field- and temperature-dependent I-V characteristics performed on a polycrystalline fiber of $Ag/YBa_2Cu_3O_{7-\delta}$ [Ag/(Y 1:2:3)].

II. EXPERIMENTAL

The Ag/(Y 1:2:3) fiber on which we reported detailed measurements here was typical of others that we have studied and was made with use of the polymer-metal-complex precursor method.[14–17] It consists of a nominal 33% Ag by weight. In the polymer-metal-complex precursor method, the reactants are mixed on the atomic level forming a polymer-metal complex and then extruded into a fiber. During a series of heat treatments, the polymer is eliminated and the reactants form the final high-T_c compound while the sample retains a fiber shape. The resulting fiber consists of "as grown" grains that are not ground nor pressed. Further details concerning the fabrication technique may be found elsewhere.[16,17]

The sample reported on here is composed of three 15-μm-diam fibers in tight contact. Scanning-electron-microscope (SEM) photographs of the sample (see Fig. 1) were taken after I-V measurements were performed. The silver appears to occur primarily as a sheath surrounding an inner fiber of granular Y 1:2:3, with smaller amounts of silver occurring in intergranular spaces. The Y 1:2:3 grains appear to be in good physical contact with few interstitial voids. Grain sizes range from ≈ 2 to 6 μm, with an average size of ≈ 4 μm. The ratio of fiber diameter to grain diameter is $d_f/d_g \sim 4$ as compared with typical values of ~ 100 for bulk pellets. The sample's low room-temperature resistivity of $\rho \approx 10$ $\mu\Omega$ cm is consistent with the silver forming a percolating sheath around the sample that dominates the normal-state conductivity. The sample had a critical current density of 510 A/cm^2 at 77 K as determined by a 1-μV/cm electric-field criterion, comparable to values measured in good-quality bulk sintered pellets. The single-grain transition temperature was $T_{c0} \approx 91.5$ K, as determined by the point in the superconducting transition at which the sample resistance is 90% of its extrapolated normal-state resistance.

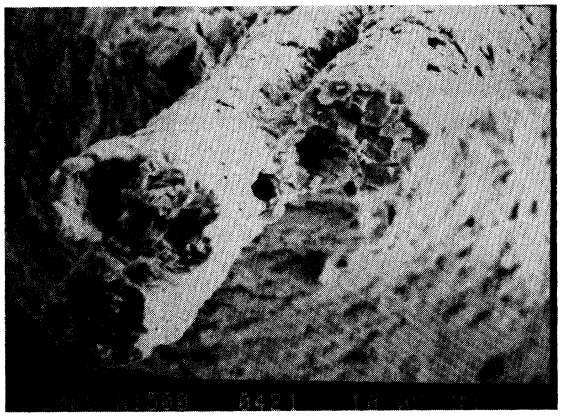

FIG. 1. Scanning-electron-microscope photograph of a cross section of the sample between the voltage contacts.

I-V curves were obtained in a ^{4}He-exchange-gas cryostat using a four-lead dc reversing-current technique. Voltage measurements were limited by voltmeter sensitivity and noise to a minimum of ≈ 0.1 μV, corresponding to an electric field of 1 μV/cm in the fiber. Due to the small cross-sectional area and low contact resistance of the fiber, we were able to produce current densities up to $\approx 2 \times 10^4$ A/cm^2, corresponding to sample currents of ≈ 100 mA. For runs performed in a magnetic field, the sample was field cooled.

Because of the percolating network of silver, in the superconducting state at $I > I_c$ a significant current may be carried by silver in parallel to current carried by Y 1:2:3. The silver current is largest at large sample voltages when $I \gg I_c$. The effect of this current on the shape of I-V curves is largest for temperatures close to T_c and for high magnetic fields because of the relatively low critical currents in these situations. The silver current is accounted for by extrapolating the normal-state resistance of the sample, which is due almost exclusively to the silver network, to the temperature of interest. The current carried by the silver is subtracted from the total current giving the current carried by Y 1:2:3 alone. This procedure was used for I-V curves at $T = 60.8$ K and above.

Systematic effects in temperature measurements caused by Joule heating of the sample were measured by observing the shift in the single-grain T_c. Sample currents of 100, 50, and 25 mA produced T_c shifts δT_c of 0.5, 0.2, and 0.02 K, respectively, at $T \approx 90$ K. These numbers provide an upper limit of δT for high-current data below T_c. The power-law I-V behavior that we report was observed for sample currents < 25 mA.

The temperature for data taken at $T = 77.0$ K was maintained by immersing the cryostat in liquid nitrogen.

For any single data run, the temperature was stable to within about 4 mK. The average temperature of all of the 77-K data runs was $T=77.0$ K with a standard deviation $\sigma=0.1$ K. Data at other temperatures were taken with the cryostat in a liquid-helium Dewar and, for a given data run, the temperature was stable to within 40 mK.

III. RESULTS AND DISCUSSION

I-V curves were obtained in the ambient field of 0.5 G at temperatures of 85.7, 77.0, 60.8, 40.7, 21.2, and 4.3 K and current densities up to 2×10^4 A/cm^2. These measurements represent a larger range of current densities than previous measurements on bulk polycrystalline high-T_c superconductors.[18] The dynamic resistance dV/dI was computed from a cubic spline fit to the *I-V* data and is shown in Fig. 2. The symbols are a convenient way to distinguish data taken at different temperatures and reflect the discrete current values at which the *I-V* data were taken. The dynamic resistance shows significant changes over this temperature range, both in the general shape of the curves and in magnitude. There is an evolution in the shape of the curves from $T=85.7$ to 60.8 K. The 85.7 K curve rises sharply at low currents and appears to be leveling off at $dV/dI\approx95$ mΩ. The 77.0-K curve rises with more or less constant slope, and the 60.8-K curve shows increasing slope over nearly the entire range of currents. The shapes of the dV/dI curves for $T\leq60.8$ K are all similar and have decreasing magnitude as the temperature is decreased. Log-log plots of dV/dI for $T\leq77.0$ K [Fig. 2(b)] are linear for $dV/dI<5$ mΩ with slopes of 3.1, 3.0, 2.4, 2.6, and 2.4 for $T=4.3$, 21.2, 40.7, 60.8, and 77.0 K, respectively. The apparent transition to dV/dI independent of current for $dV/dI\sim10$ mΩ and $T\leq40.7$ K is an artifact due to current through the silver percolating network. We were unable to accurately estimate the resistance of the Ag network at these temperatures.

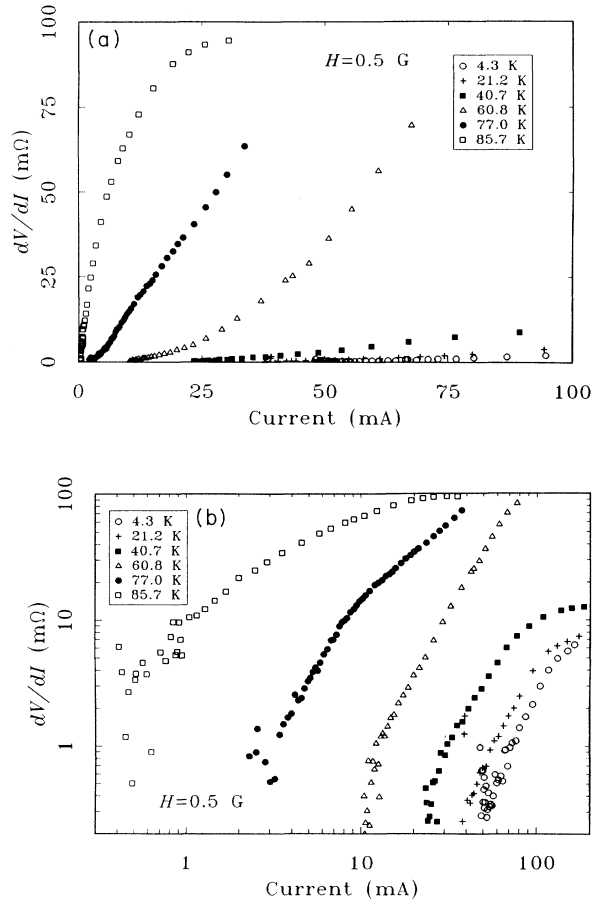

FIG. 2. (a) Dynamic resistance dV/dI vs I for $H=0.5$ G and $T=4.3$, 21.2, 40.7, 60.8, 77.0, and 85.7 K. Currents for $T\geq60.8$ K were limited by Joule heating and at the highest-current levels most current was shunted by the percolating silver network. (b) Same data on a log-log scale. A 1-mA current corresponds to a 200-A/cm^2 current density.

Figure 3 shows plots of V versus $I-I_c$ on a log-log scale for the various temperatures. The *I-V* data were fitted with a power law of the form $V=K(I-I_c)^a$ for $V\leq8$ μV using a nonlinear least-squares fitting routine. The data for $40.7\leq T\leq85.7$ K fit the power law, but at $T=4.3$ and 21.2 K the curves showed systematic departures from power-law behavior. Table I lists relevant parameters for these data. $I_c^{\rm fit}$ is the I_c fit parameter in the $V=K(I-I_c)^a$ fits. In addition, an effective critical current $I_c^{\rm eff}$ was found by measuring the sample current at a 1-μV/cm sample electric field. Both critical currents rise approximately linearly with decreasing temperature for $T\leq60.8$ K. $H(I_c,r)$ gives the computed field produced at the surface of the sample by $I_c^{\rm fit}$. For $T\leq60.8$ K, this field is greater than the ambient field.

The parameter γ is the ratio of $(\hbar/2e)\langle I_{cJ}\rangle$ to the thermal energy k_BT, where $\langle I_{cJ}\rangle$ is the average single-junction critical current, $\langle I_{cJ}\rangle=I_cd_g^2/A_s$. d_g is the average grain diameter and A_s is the cross-sectional area of the sample. As mentioned before, an operational critical current, such as $\langle I_{cJ}\rangle$, that marks the onset of measur-

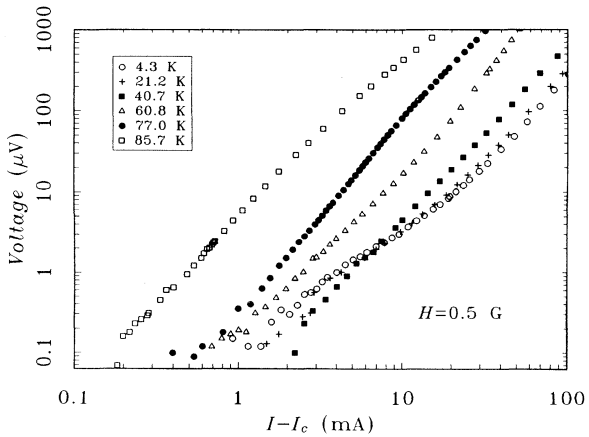

FIG. 3. V vs $I-I_c$ for $H=0.5$ G and $T=4.3$, 21.2, 40.7, 60.8, 77.0, and 85.7 K. A voltage of 1 μV corresponds to a 10-μV/cm electric field.

TABLE I. Parameters for *I-V* curves at $H=0.5$ G and various temperatures. $I_c^{\rm eff}$ is an effective critical current determined by the sample current at a 1-μV/cm sample electric field. $I_c^{\rm fit}$ and a are power-law fit parameters. $H(r,I_c)$ is the field at the surface of the fiber produced by $I_c^{\rm fit}$. $\gamma=(\hbar/2e)\langle I_{cJ}\rangle/k_BT$, where $\langle I_{cJ}\rangle$ is the average junction critical current. $I_c^{\rm fit}$ values enclosed by parentheses were used to obtain the plots of Fig. 3 for temperatures that did not obey the power law.

T (K)	$I_c^{\rm eff}$ (mA)	$I_c^{\rm fit}$ (mA)	a	$H(r,I_c^{\rm fit})$ (G)	γ
4.3	47.8	(47)		4.0	7500
21.2	37.0	(36)		3.1	1200
40.7	23.0	21.2	2.1	1.9	370
60.8	10.5	9.7	1.9	0.85	110
77.0	2.7	2.0	2.4	0.18	19
85.7	0.41	0.23	2.3	0.02	1.9

able voltage is less than the Josephson critical current $\langle I_{ij}\rangle$ as a result of thermal fluctuations. γ as listed in Table I gives a lower bound on the ratio $\langle E_{ij}\rangle/k_BT$. The phase-locking transition should occur at $k_BT_c\sim\langle E_{ij}\rangle$.

I-V curves were also obtained in magnetic fields ranging from 0.5 to 9000 G at a fixed temperature of 77.0 K. These measurements represent a larger range of current densities as well as a larger range and a more thorough coverage of magnetic fields than previous field-dependent *I-V* studies done on bulk polycrystalline high-T_c superconductors.[18,19] Selected plots of dV/dI versus I calculated from cubic spline fits to this data are shown in Figs. 4(a) and 4(b). As was the case in Fig 2, the data points indicate the current values at which *I-V* measurements were taken. There is a progressive change in the nature of the dV/dI curves for $0.5\le H\le 9$ G. The $H=0.5$ G curve shows no sign of leveling off at the highest currents studied, with dV/dI rising smoothly over the full range of currents explored. Increasing field produces more curvature in dV/dI until at $H=9$ G dV/dI has clearly leveled off at $I\sim 40$ mA. For $H\gtrsim 9$ G, dV/dI levels off at a weakly field-dependent value $\lesssim 70$ mΩ. The value of dV/dI in this linear regime is expected to be due to the resistance of grain boundaries. From the sample dimensions and average grain size, the observed value of 70 mΩ indicates an average grain-boundary resistance $\langle r_n\rangle\approx 10$ mΩ. This is similar to the value of $\langle r_n\rangle\approx 20$ mΩ reported by Bungre *et al.*[18] for a Y 1:2:3 bulk sintered pellet.

The *I-V* curves for $H\gtrsim 9$ G have a similar shape as they change from nonlinear to linear behavior with increasing current. This is illustrated with plots of dV/dI versus $I/I_0(H)$ shown in Fig. 5. $I_0(H)$ is defined to be the current at which $dV/dI=60$ mΩ, about 90% of the maximum value of dV/dI for a given field. A plot of $I_0(H)$ is shown in Fig. 6. $I_0(H)$ for $6\le H\le 28$ G gives a straight line on a log-log scale, and a nonlinear least-squares fit of this data to the form $I_0\propto H^n$ gives $n=-1.18\pm 0.05$. This $I_0\sim 1/H$ field dependence may be related to the single-Josephson-junction field dependence of $I_{cJ}(H)\propto|\sin(H/H_0)|/(H/H_0)|$, where I_{cJ} is the Josephson critical current in a single junction neglecting the effects of thermal fluctuations.[20] I_0 falls less steeply for $H\gtrsim 50$ G, but is still linear on a log-log scale. For $80\le H<\le 9000$ G, a nonlinear least-squares fit to $I_0\propto H^n$ gives $n=-0.32\pm 0.05$. We are not aware of an explanation for the $I_0\sim H^{-1/3}$ field dependence, but the leveling off of I_0 with increasing field may be attributable to a leveling off of grain-boundary fields due to flux relaxing from grain-boundary regions into grains above H_{c1}. The lowest H_{c1} for Y 1:2:3 is ≈ 60 G at $T=77.0$ K.

It is interesting to compare the results shown in Figs. 4

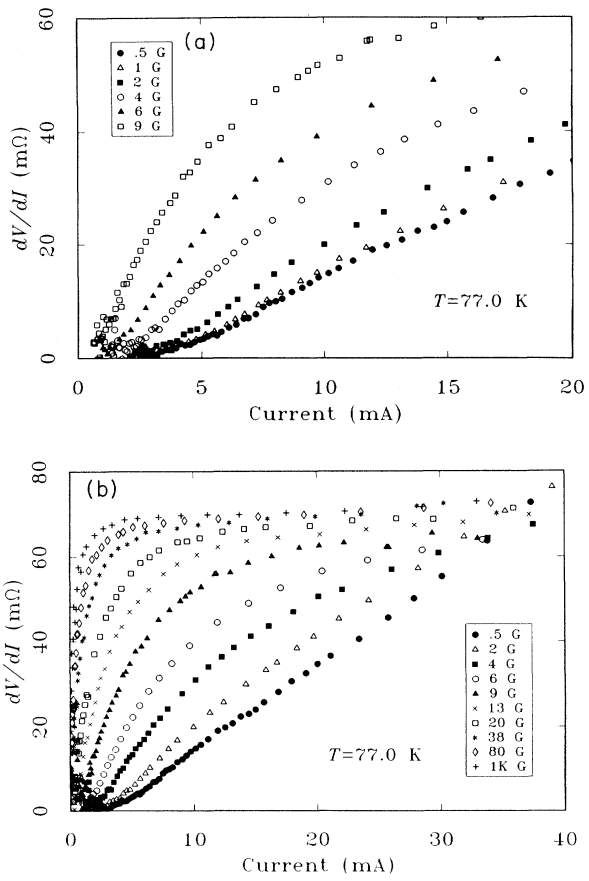

FIG. 4. Dynamic resistance dV/dI vs I for $T=77.0$ K and selected values of H. (a) $0.5\le H\le 9$ G. (b) $0.5\le H\le 1000$ G. A 1-mA current corresponds to a 200-A/cm^2 current density.

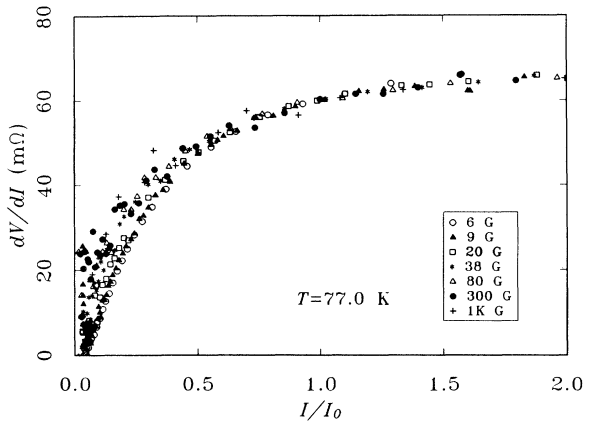

FIG. 5. Dynamic resistance vs I/I_0. I_0 is the current at which $dV/dI = 60$ mΩ for a given field.

and 5 with recent measurements on a fabricated two-dimensional Josephson-junction array.[7] In zero field, the array exhibited a crossover from nonlinear to linear I-V characteristics. The crossover was marked by a peak of dV/dI that was interpreted to mark the point at which the current through each junction equaled the Josephson critical current I_{ij}. In small applied fields, the original dV/dI peak was reduced and broadened and an additional similar peak at roughly $\frac{1}{2}I_{ij}$ was observed. This new peak was interpreted to mark a flux depinning critical current I_{cB}. I_{cB} is the current at which integranular flux vortices can be driven across the sample in the absence of thermal fluctuations.

The crossover from nonlinear to linear behavior seen in Fig. 4 suggests a similar phenomenon. Because of the randomness in coupling energies and grain sizes and also the relatively large ratio of grain diameter to sample diameter, there is probably a range of flux-depinning critical currents over the length of the sample. As a result, the crossover should not be as sharp as for a regular array. Applying the interpretation of Benz *et al.*[7] to the dynamic resistance data shown in Figs. 4 and 5 suggests that I_0 represents an average intergranular flux-depinning critical current. The nonlinear region near the onset of a measurable voltage is due to a thermally assisted "creep" of intergranular flux vortices across the sample and the crossover to linear I-V characteristics is due to a change from flux creep to flux flow.

It is likely that the evolution of the dV/dI curves seen in Fig. 4 between $H = 0.5$ and 9 G results from the increasing importance of integranular flux motion with increasing field in this region. For $H \lesssim 1$ G, the number of intergranular vortices may be small enough that the voltage produced by thermal phase slippage is comparable to flux-creep voltage. To see if this is a reasonable hypothesis, we next estimate the relationship between H and the amount of flux available for intergranular flux creep. The region of grain-boundary flux creep should extend a distance of the magnetic penetration depth λ on either side of the grain boundary. Averaging over the three crystal directions and using $\lambda_a \approx \lambda_b \approx 2200$ Å and $\lambda_c \approx 7800$ Å at $T = 77$ K (Ref. 21) gives an average penetration depth $\langle\lambda\rangle \approx 4000$ Å. This is $\approx \frac{1}{10}$ of the average grain size d_g. This sample was field cooled; and, for $H < H_{c1}$, field-cooled grains exhibit a partial Meissner effect, with the Meissner fraction depending on H.[22,23] For $H \leq 1$ G a Meissner fraction of $\lesssim 50\%$ is expected, indicating that roughly 50% of the flux is expelled from the grains. Between 1 and 30 G the Meissner fraction should fall from $\sim 50\%$ to $\sim 10\%$. As a result, the magnetic field in the grain-boundary region, B_{GB}, should be $H \leq B_{GB} \leq 2H$ for $H \leq 50$ G, and accordingly there is one flux quantum ($\phi_0 = hc/2e$) per gain boundary at a field of $H = 3$–6 G. From this, it is reasonable to expect that, for $H \ll 5$ G, intergranular flux creep is a small effect, whereas, for $H \gtrsim 5$ G, flux creep should become increasingly important. This is in agreement with the data of Fig. 4.

Figure 7 shows V versus $I - I_c$ data at selected fields.

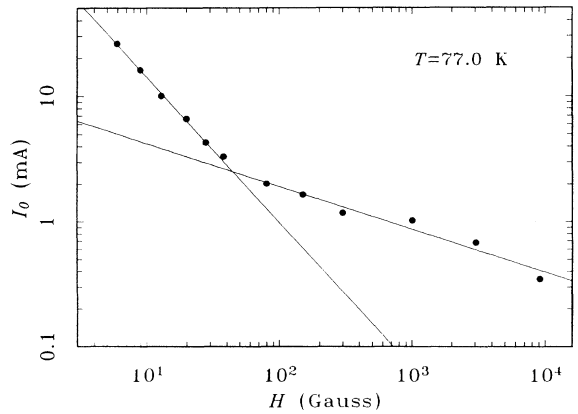

FIG. 6. I_0 vs H. I_0 is the current at which $dV/dI = 60$ mΩ for a given field. Lines show fits discussed in the text.

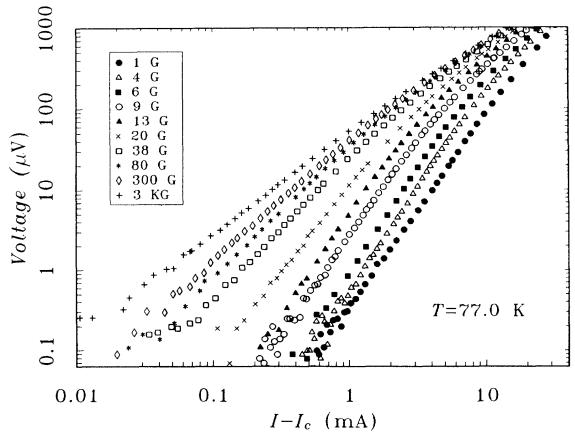

FIG. 7. V vs $I - I_c$ for $T = 77.0$ K and selected field values for $1 \leq H \leq 3000$ G. A voltage of 1 μV corresponds to a 10-μV/cm electric field.

At low currents near the onset of measurable voltage, these data obey the power law $V=K(I-I_c)^a$ for about two decades in voltage over the entire range of magnetic fields. Based on the preceding discussion of dV/dI data, this power-law behavior is due mainly to thermally assisted flux creep for $H \gtrsim 6$ G and a combination of flux creep and thermal phase slippage for $H < 6$ G.

The I-V power-law is in general agreement with predictions of a two-dimensional Josephson-junction-array superconducting glass model.[24] This model predicts $V=K(I_s-I_c)^a$ power-law behavior, where I_s is the current of superconducting electrons. The functional form of I-V curves depends on the time dependence of the phase correlation function $D(t)$, which gives the time decay of superconducting phase coherence between grains. In the superconducting glass model, power-law I-V characteristics are due to power-law relaxation in $D(t)$ of the form $D(t)=L+D_0(t/\tau)^{-\alpha}$, with $L \propto I_c$, $D_0 \propto 1/K$, and $\alpha=1/a$. Sergeenkov[24] proposes a functional form for α that gives $a=2$ at T_c and then rising for $T < T_c$. He further predicts a field dependence for a characterized by $a \geq 2$ for $H \approx 0$ and $T < T_c$, then falling with increasing field. The vanishing of I_c is predicted to coincide with $a=2$. Possible values of $a(T_c)$ have been discussed by Lebeau *et al.*[25] for three-dimensional Josephson-junction arrays. They predict $a(T_c)=2$ based on hyperscaling arguments and $a(T_c)=\frac{3}{2}$ for high enough fields based on a time-dependent Ginzburg-Landau treatment. Our data are in qualitative agreement with Sergeenkov's predictions of the field dependence of a, but show a vanishing of I_c coincident with $a \approx 1.5$ at $T=77.0$ K and $H \sim 1000$ G, as we next illustrate.

The fit parameters I_c, a and K determined from nonlinear least-squares fits to the data of Fig. 7 for $V \leq 8$ μV show an interesting field dependence, as can be seen in Figs. 8–10. The error bars represent a 1σ confidence interval. For $H \lesssim 2$ G, all three fit parameters are constant. For H increasing in the range $2 \lesssim H \lesssim 6$ G, I_c begins to decrease and K and a begin to rise. For $10 \lesssim H \lesssim 50$, all three parameters decrease sharply. For $H \gtrsim 50$ G, I_c gradually drops to a value consistent with zero at $1000 \leq H \leq 3000$ G, while K and a decrease gradually. The exponent a falls sharply with $H(G)$ for $10 \leq 50$ G and decreases gradually through $a \approx 1.5$, coincident with $I_c \rightarrow 0$.

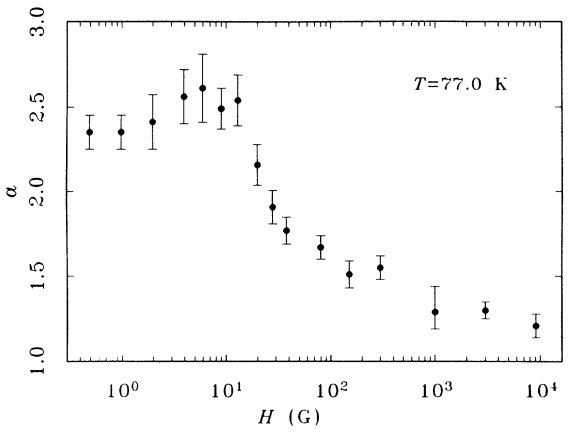

FIG. 9. Power-law fit parameter a vs H.

If I_0 determined from the dV/dI plots and shown in Fig. 6 is an average flux-depinning critical current, then differences between I_0 and $I_c^{\rm fit}$ gauge the relative importance of thermal fluctuations as compared to grain-coupling-energy disorder in determining the I-V characteristics of the nonlinear I-V region. I_0 and I_c have a similar field dependence, and the ratio I_0/I_c rises roughly linearly from about 50 at $H \sim 10$ G to about 100 at $H \sim 500$ G. In order to gauge the relative importance of disorder to thermal fluctuations it is necessary to determine an energy associated with a given current. In an ordered two-dimensional Josephson-junction array, intergranular vortices see a periodic potential with barrier height $E_B \approx (\hbar/e) i_{cB}$ where i_{cB} is the vortex-depinning current per single junction.[26] In a random three-dimensional Josephson-junction array, any given path that a vortex can take across the sample has an associated

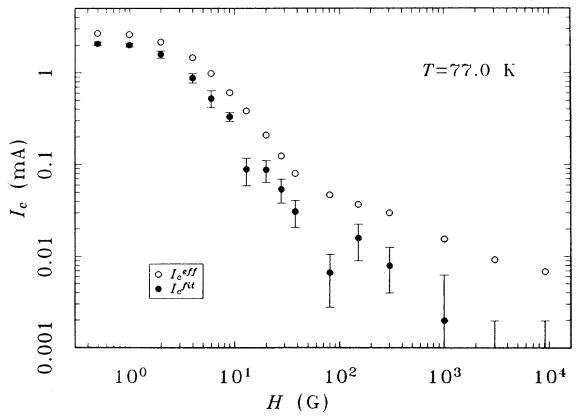

FIG. 8. Power-law fit parameter $I_c^{\rm fit}$ and the effective critical current $I_c^{\rm eff}$ vs H. The lower error bar for $H=1000$ includes $I_c=0$.

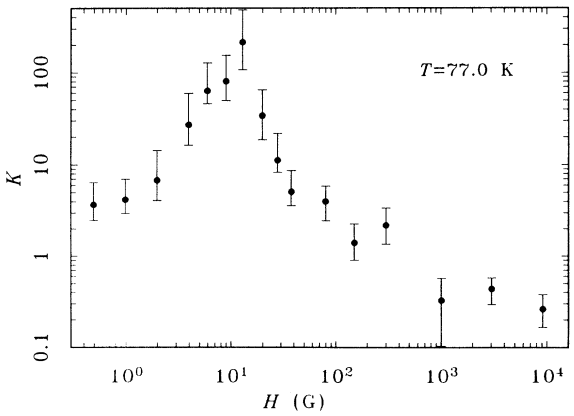

FIG. 10. Power-law fit parameter K vs H.

effective barrier height. Generalizing the two-dimensional result gives for a single vortex path an effective barrier height $E_B \sim (\hbar/e) I_{cB} lb/A_s$. I_{cB} is the depinning sample current for that particular vortex path, l is the effective length of the vortex, b is the average distance between potential barriers, and A_s is the sample cross-sectional area. Taking $b = l = d_g$ with d_g the average grain size gives an approximate lower limit for E_B of $E_0 = (\hbar/e) I_{cB} d_g^2 / A_s$. If the range of barrier heights associated with the possible flux paths is less than, or comparable to, $k_B T$, then $E_0(I_0)$ should be $\sim k_B T$ above $E_0(I_c)$. If, on the other hand, the range of barrier heights is much greater than $k_B T$, then the difference between $E_0(I_0)$ and $E_0(I_c)$ will also be much larger than $k_B T$ and reflect the range of energy barriers. At $H = 9$ G, $E_0(I_0)/k_B = 23\,100$ K, $E_0(I_c)/k_B = 480$ K, and $[E_0(I_0) - E_0(I_c)]/k_B T = 290$. These numbers suggest that, for $H = 9$ G, disorder and the resulting energy hierarchy of available flux paths play a key role in producing the observed nonlinear I-V characteristics. For $H = 300$ G, the highest measured field with a definite nonzero I_c, $E_0(I_0)/k_B = 1990$ K, $E_0(I_c)/k_B = 115$ K, and $[E_0(I_0) - E_0(I_c)]/k_B T = 24$. These numbers suggest that thermal effects play an increasing role with increasing field. For $1000 \lesssim H \lesssim 3000$ G, $I_c^{\rm fit}$ drops to a value consistent with zero. The vanishing of $I_c^{\rm fit}$ G may indicate that the field-induced drop in $\langle I_{ij} \rangle$ is such that $\langle E_{ij} \rangle \sim k_B T$, resulting in a suppression of intergranular phase coherence by thermal fluctuations. The fact that, for $H = 300$ G, $E_0(I_c)/k_B$ is close to the actual temperature supports this hypothesis.

The decrease in the magnitude of the slope of both I_c and I_0 that occurs for $H \gtrsim 80$ G coincides with one of the single-grain lower critical fields H_{c1}. This may arise from a leveling off of the grain-boundary magnetic field as flux relaxes from grain boundaries into grains above H_{c1}, or could signal changes in intergranular flux dynamics associated with H_{c1}. Y 1:2:3 has two critical fields due to its anisotropy. At 77 K, $H_{c1} \approx 60$ G for **H** parallel to the a or b crystal axis and $H_{c1} \approx 180$ G for **H** parallel to the c axis and $H_{c1} \approx 180$ G for **H** parallel to the c crystal axis.[21]

For a single Josephson junction, a magnetic field perpendicular to the direction of junction current causes a reduction in critical current as[20]

$$I_{cJ}(H) = I_{cJ}(0) \frac{|\sin(\pi\phi/\phi_0)|}{\pi\phi/\phi_0} . \quad (1)$$

I_{cJ} is the Josephson critical current neglecting effects of thermal fluctutations, ϕ is the magnetic flux penetrating the junction, and $\phi_0 = hc/2e$. This equation has been used to explain the functional form of $I_c(H)$ in polycrystalline Y 1:2:3 by comparing the measured $I_c(H)$ with a calculated $I_c(H)$ for a random ensemble of Josephson junctions that obey Eq. (1).[2] This approach predicts results that are consistent with the behavior that we observe for both $I_c(H)$ and $I_0(H)$ for $H \lesssim 50$ G. From the previous considerations though, it appears that this approach is an oversimplification of the real situation. The onset of measurable voltage arises from both phase slip and flux creep for $H \lesssim 1$ G, whereas, for $H \gtrsim 6$ G, flux creep alone dominates. In addition, even for $H \gtrsim 9$ G, the behavior of $I_c(H)$ is not uniform, but can be separated into three regions: $6 \lesssim H \lesssim 30$ G, where I_0 and $I_c(H) \sim 1/H$; $50 \lesssim H \lesssim 300$ G, where I_0 and $I_c(H)$ have a weaker dependence on H; and $H \gtrsim 1000$ G, where I_c apparently vanishes.

Possible effects due to intergranular flux flow as well as effects due to differences between the grain-boundary magnetic field $B_{\rm GB}$ and H can be investigated from differences in the I-V data of field-cooled (FC) and zero-field-cooled (ZFC) samples. FC and ZFC sample voltages at a fixed current of 1 mA were measured for $0.5 \lesssim H \lesssim 9000$ G at $T = 77.5$ K. See Fig. 11. The ratio $V_{\rm ZFC}/V_{\rm FC}$, shown in the inset of Fig. 11, appears to be relatively constant below 200 G and to fall above 300 G.

As was discussed earlier, below H_{c1} FC and ZFC samples are expected to have different distributions of flux that may give rise to different I-V behavior. FC samples should have some fraction of flux pinned in grains with a larger flux density at grain boundaries, whereas for ZFC samples virtually all flux is confined to grain-boundary regions. Intragranular flux is pinned at $T = 77.0$ K for the entire range of magnetic field and current that was explored in this sample. Accordingly, the different voltages observed for field cooling and zero field cooling seen in Fig. 11 are probably due to differences in the number of intergranular flux vortices available for flux creep. This argument has been used recently to explain differences in the microwave surface resistance of FC and ZFC polycrystalline Y 1:2:3 samples over a similar field and temperature region.[27] For $H \gg H_{c1}$, the flux distributions of FC and ZFC samples should both be uniform, and as a result FC and ZFC voltages should be identical. These observations are in agreement with Fig. 11.

The data shown in Fig. 11 represent a cut through several different regions of I-V behavior and illustrate the different characteristics of these regions. For $H \lesssim 5$ G, there is no measurable sample voltage. For $10 \lesssim H \lesssim 50$ G, the sample is in the nonlinear power-law regime and $V(H)$ rises sharply. The decrease in dV/dH at $H \sim 100$ G coincides with the change in behavior of I_c, a, and K

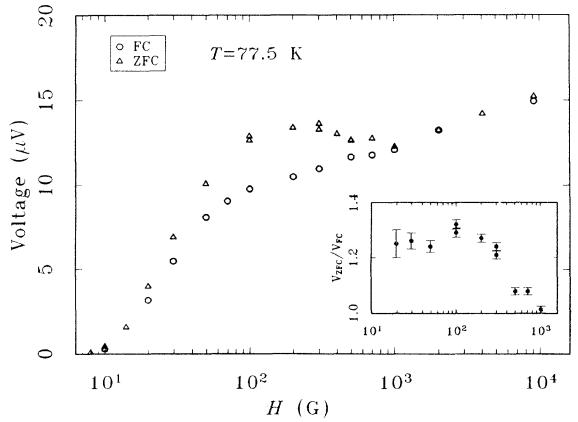

FIG. 11. Field-cooled and zero-field-cooled sample voltages vs magnetic field at a fixed current of 1 mA and $T = 77.5$ K. Inset gives the ratio of zero-field-cooled to field-cooled voltages vs field.

that occurs near the lowest H_{c1} (see Figs. 7–10). At $T=77.0$ K, the crossover currents I_0 for fields of 80 and 1000 G are 2.0 and 1.0 mA, respectively. The data for $50 \lesssim H \lesssim 1000$, then are representative of the nonlinear to linear crossover region and the data for $H \gtrsim 1000$ G are representative of the linear I-V region.

The most surprising aspect of Fig. 11 is the drop in ZFC voltage between 300 and 1000 G. These field values are $\approx 2-5$ times greater than the highest H_{c1} value, and the drop in voltage is probably due to the process of flux relaxing from grain-boundary regions into the grains themselves. Although the number of flux vortices in any grain boundary is not expected to decrease with increasing field, the number of vortices that pass *exclusively* through grain-boundary regions will decrease at some field.

Based on the changes seen in Fig. 11 for $80 \leq H \leq 1000$ G, as well as the previously discussed changes in power-law parameters and I_0 that occur near 80 G, changes in flux distribution or dynamics associated with the lower critical fields apparently cause significant changes in the mobility of intergranular vortices.

IV. CONCLUSION

We have investigated the I-V characteristics of an Ag/(Y 1:2:3) polycrystalline fiber and their dependence on temperature and magnetic field. These measurements represent a wider range of current densities and magnetic fields as well as a more complete coverage of fields than previous studies done on bulk polycrystalline samples and reveal a complex variety of behavior. Measurements at $H=0.5$ G and $4.3 \leq T \leq 85.7$ show significant changes in the shapes of the I-V curves between 85.7 and 60.8 K, whereas I-V curves for $T \leq 60.8$ K all have a similar shape. Nonlinear I-V behavior was seen near the onset of measurable voltages for all of these data, and for $40.7 \leq T \leq 85.7$ K these nonlinear I-V curves obey a power law over two decades of voltage. The I-V curves for $0.5 \leq H \leq 9000$ G and $T=77.0$ K exhibit a variety of changes with field and current, all of which are generally consistent with behavior expected from a system of weakly coupled superconducting grains. Our data indicate the increasing importance of intergranular flux motion on I-V characteristics for $0.5 \leq H \leq 9$ G and also reveal a crossover from nonlinear to linear I-V behavior with increasing current for $H \geq 9$ G associated with a transition from flux creep to flux flow. Near the onset of measurable voltage and for all fields the I-V curves obeyed a power law. The field dependence of the power-law exponent a is in qualitative agreement with predictions of Sergeenkov,[24] although the vanishing of I_c coincides with $a \approx 1.5$, rather than with $a=2$ as proposed by Sergeenkov. Comparisons of I_0, I_c, and the inferred energy barriers suggest that grain-coupling energy disorder plays a key role in producing the observed nonlinear I-V characteristics. Field-dependent changes in the dynamic resistance, power-law parameters, and crossover current indicate the existence of several distinct regions of field-dependent behavior and also suggest changes in intergranular flux motion related to the single-grain lower critical fields.

ACKNOWLEDGMENTS

We thank J. C. W. Chien, B. M. Gong, and Y. S. Yang for providing us with the sample and SEM photographs. This work was supported by Research Trust Funds administered by the University of Massachusetts and to a limited extent by NSF Grant No. DMR 88-20517.

[1] J. F. Kwak, E. L. Venturini, P. J. Nigrey, and D. S. Ginley, Phys. Rev. B **37**, 9749 (1988).
[2] R. L. Peterson and J. W. Ekin, Phys. Rev. B **37**, 9848 (1988).
[3] P. Chaudhari, J. Mannhart, D. Dimos, C. C. Tsuei, J. Chi, M. M. Oprysko, and M. Scheuermann, Phys. Rev. Lett. **60**, 1653 (1988).
[4] D. Dimos, P. Chaudhari, J. Mannhart, and F. K. LeGoues, Phys. Rev. Lett. **61**, 219 (1988).
[5] J. R. Clem, Physica B+C **153-155C**, 50 (1988).
[6] M. Tinkham and C. J. Lobb, Solid State Physics: *Advances in Research and Applications,* edited by H. Ehrenreich and D. Turnbull (Academic, New York, 1989), Vol. 42, p. 91.
[7] S. P. Benz, M. S. Rzchowski, M. Tinkham, and C. J. Lobb, Phys. Rev. B **42**, 6165 (1990).
[8] V. Ambegaokar and B. I. Halperin, Phys. Rev. Lett. **22**, 1364 (1969).
[9] M. Simmonds and W. H. Parker, Phys. Rev. Lett. **24**, 876 (1970).
[10] M. A. Dubson, S. T. Herbert, J. J. Calabrese, D. C. Harris, B. R. Patton, and J. C. Garland, Phys. Rev. Lett. **60**, 1061 (1988).
[11] P. England, T. Venkatesan, X. D. Wu, and A. Inam, Phys. Rev. B **38**, 7125 (1988).
[12] H. E. Horng, J. C. Jao, H. C. Chen, H. C. Yang, H. H. Sung, and F. C. Chen, Phys. Rev. B **39**, 9628 (1989).
[13] J. Jung, M. A.-K. Mohamed, S. C. Cheng, and J. P. Franck, Phys. Rev. B **42**, 6181 (1990).
[14] W. M. Tiernan, J. M. Madsen, R. B. Hallock, J. C. W. Chien, B. M. Gong, S. H. Dong, and Y. S. Yang, Physica B+C **168C**, 189 (1990).
[15] W. M. Tiernan, R. B. Hallock, J. C. W. Chien, B. M. Gong, S. H. Dong, and Y. S. Yang, in *Proceedings of the 19th International Conference on Low Temperature Physics* [Physica B+C **165-166B**, 1383 (1990)].
[16] J. C. W. Chien, B. M. Gong, J. M. Madsen, and R. B. Hallock, Phys. Rev. B **38**, 853 (1988).
[17] J. C. W. Chien, B. M. Gong, X. Mu, and Y. S. Yang, J. Polym. Sci. Part A **28**, 1999 (1990).
[18] S. S. Bungre, R. Meisels, A. D. Caplin, and S. E. Male, Physica B+C **162-164C**, 1171 (1989).
[19] J. E. Evetts, B. A. Glowacki, P. L. Sampson, M. G. Blamire, N. M. Alford, and M. A. Harmer, IEE Trans. Magn. **25**, 2041

(1989).
[20]T. Van Duzer and C. W. Turner, *Principles of Superconductive Devices and Circuits* (Elsevier, New York, 1981), Chap. 4.
[21]L. Krusin-Elbaum, A. P. Malozemoff, Y. Yeshurun, D. C. Cronemeyer, and F. Holtzberg, Phys. Rev. B **39**, 2936 (1989).
[22]L. Krusin-Elbaum, A. P. Malozemoff, Y. Yeshuruin, D. C. Cronemeyer, and F. Holtzberg, Physica B+C **153-155C**, 1469 (1988).
[23]A. P. Malozemoff, L. Krusin-Elbaum, D. C. Cronemeyer, Y. Yeshuruin, and F. Holtzberg, Phys. Rev. B **38**, 6490 (1988).
[24]S. A. Sergeenkov, Physica B+C **167C**, 339 (1990).
[25]C. Lebeau, J. Rosenblatt, A. Raboutou, and P. Peyral, Europhys. Lett. **1**, 313 (1986).
[26]M. S. Rzchowski, S. P. Benz, M. Tinkham, and C. J. Lobb, Phys. Rev. B **42**, 2041 (1990).
[27]L. Ji, M. S. Rzchowski, and T. Tinkham, Phys. Rev. B **42**, 4838 (1990).

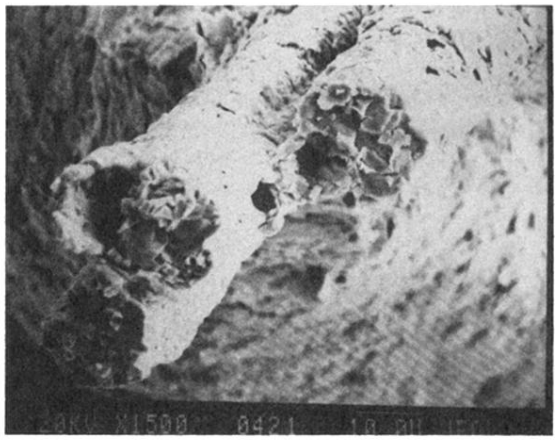

FIG. 1. Scanning-electron-microscope photograph of a cross section of the sample between the voltage contacts.